# Journal Pre-proof

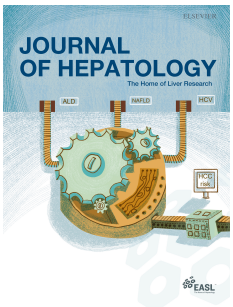


Claudin-1 is a mediator and therapeutic target in primary sclerosing cholangitis

Fabio Del Zompo, Emilie Crouchet, Tessa Ostyn, Zeina Nehme, Mélissa Messé, Frank Juehling, Romain Désert, Angelica T. Vieira, Julien Moehlin, Diana Nakib, Tallulah Andrews, Catia Perciani, Sai Chung, Gary Bader, Ian McGilvray, Chiara Caime, Miki Scaravaglio, Marco Carbone, Pietro Invernizzi, Sheraz Yaqub, Trine Folseraas, Tom H. Karlsen, Gautam Shankar, Mark Primeaux, Punita Dhawan, Jesus M. Banales, Natascha Roehlen, Roberto Iacone, Geoffrey Teixeira, Mathias Heikenwälder, Laurent Mailly, Sonya MacParland, Tania Roskams, Olivier Govaere, Catherine Schuster, Thomas F. Baumert

PII: S0168-8278(25)02440-7

DOI: https://doi.org/10.1016/j.jhep.2025.08.005

Reference: JHEPAT 10229

To appear in: *Journal of Hepatology*

Received Date: 13 September 2024

Revised Date: 9 July 2025

Accepted Date: 5 August 2025

Please cite this article as: Del Zompo F, Crouchet E, Ostyn T, Nehme Z, Messé M, Juehling F, Désert R, Vieira AT, Moehlin J, Nakib D, Andrews T, Perciani C, Chung S, Bader G, McGilvray I, Caime C, Scaravaglio M, Carbone M, Invernizzi P, Yaqub S, Folseraas T, Karlsen TH, Shankar G, Primeaux M, Dhawan P, Banales JM, Roehlen N, Iacone R, Teixeira G, Heikenwälder M, Mailly L, MacParland S, Roskams T, Govaere O, Schuster C, Baumert TF, Claudin-1 is a mediator and therapeutic target in primary sclerosing cholangitis, *Journal of Hepatology*, https://doi.org/10.1016/j.jhep.2025.08.005.

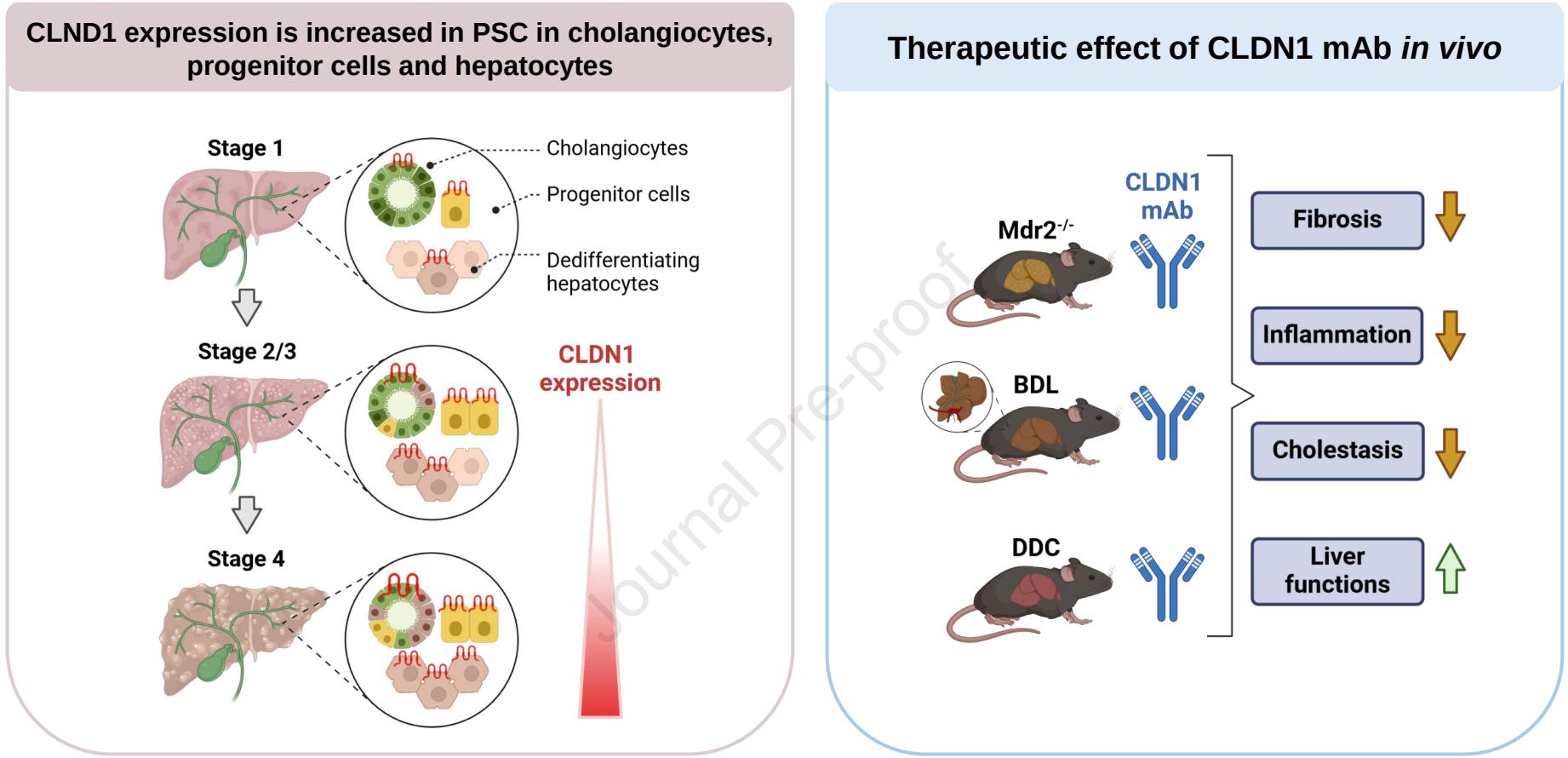

# Claudin-1 is a mediator and therapeutic target in primary sclerosing cholangitis

Fabio Del Zompo[1], Emilie Crouchet[1], Tessa Ostyn[2], Zeina Nehme[1], Mélissa Messé[1], Frank Juehling[1], Romain Désert[1], Angelica T. Vieira[1], Julien Moehlin[1], Diana Nakib[3,4], Tallulah Andrews[3,4] , Catia Perciani[3,4], Sai Chung[3,4], Gary Bader[5], Ian McGilvray[4], Chiara Caime[6,7], Miki Scaravaglio[6,7], Marco Carbone[7,8], Pietro Invernizzi[6,7], Sheraz Yaqub[9], Trine Folseraas[10], Tom H. Karlsen[10], Gautam Shankar[2,11], Mark Primeaux[12], Punita Dhawan[12], Jesus M. Banales[13,14], Natascha Roehlen[1,§], Roberto Iacone[15], Geoffrey Teixeira[15], Mathias Heikenwälder[16,17], Laurent Mailly[1], Sonya MacParland[3,4], Tania Roskams[2], Olivier Govaere[2], Catherine Schuster[1],

Thomas F. Baumert[1,18,19,20 *]

[1]Inserm U1110, Institute of Translational Medicine and Liver Diseases (ITM), University of Strasbourg, Strasbourg, France; [2]Department of Imaging and Pathology, KU Leuven and University Hospitals Leuven, Leuven, Belgium; [3]Department of Immunology, University of Toronto, Toronto, Canada; [4]Ajmera Transplant Center, University Health Network, Toronto, Canada; [5]Donnelly Centre for Cellular and Biomolecular Research, University of Toronto, Toronto, Canada; [6]Division of Gastroenterology, Center for Autoimmune Liver Diseases, European Reference Network on Hepatological Diseases (ERN RARE-LIVER), Fondazione IRCCS San Gerardo dei Tintori, Monza, Italy; [7]Department of Medicine and Surgery, University of Milano-Bicocca, Milan, Italy; [8]Hepatology and Gastroenterology Unit, ASST Grande Ospedale Metropolitano

Niguarda, Milan, Italy; [9]Department of Hepatobiliary Surgery, Oslo University Hospital and Institute of Clinical Medicine, University of Oslo, Norway. [10]Norwegian PSC Research Center (NoPSC), Oslo, Norway; [11] KU Leuven Institute for Single Cell Omics (LISCO), KU Leuven, Leuven, Belgium; [12] Department of Biochemistry and Molecular Biology, University of Nebraska Medical Center, Omaha, NE, USA; [13]Department of Liver and Gastrointestinal Diseases, Biogipuzkoa Health Research Institute – Donostia University Hospital, University of the Basque Country (UPV/EHU), CIBERehd, Ikerbasque, 20014, San Sebastian, Spain; [14]Department of Biochemistry and Genetics, School of Sciences, University of Navarra, Pamplona; [15] Alentis Therapeutics, Allschwil, Switzerland; [16] Division of Chronic Inflammation and Cancer, German Cancer Research Center Heidelberg, Heidelberg, Germany; [17] M3 Research Institute, Medical Faculty Tuebingen (MFT), Tuebingen, Germany; [18] IHU Strasbourg, France; [19] Gastroenterology and Hepatology Service, Strasbourg University Hospitals, Strasbourg, France, [20] Institut Universitaire de France, Paris, France.

[§] Present address: Department of Medicine II, Gastroenterology, Hepatology, Endocrinology and Infectious Diseases, Freiburg University Medical Center, Faculty of Medicine, University of Freiburg, Freiburg, Germany; Berta-Ottenstein-Programme, Faculty of Medicine, University of Freiburg, Freiburg, Germany.

*Correspondence to: Prof. Thomas F. Baumert, MD, Inserm U1110, ITM, University of Strasbourg, 3 Rue Koeberlé, 67000 Strasbourg, France, phone (+33) 3365583703, e-mail: thomas.baumert@unistra.fr

**Short title**

CLDN1 and primary sclerosing cholangitis

**Conflict of Interest**

Inserm, the University of Strasbourg, the Strasbourg University Hospitals and Alentis Therapeutics have filed a patent application for the use of anti-claudin-1 antibodies to treat cholangiopathies (PCT/IB2023/055666). TFB is founder, shareholder, consultant of Alentis. CS is shareholder of Alentis. GT and RI are employees of Alentis.

**Author contributions**

T.F.B. initiated and coordinated the study. F.D.Z. and T.F.B. designed or performed experiments and analyzed data. T.O., O.G., T.R., C.C., M.S., M.C., P.I., F.D.Z. performed CLDN1 expression analyses of human PSC tissues by IHC or immunofluorescence. T.O., G.S., O.G., T.R. performed multiplex iterative labelling by antibody neodeposition (MILAN) studies. F.D.Z., Z.N., M.M., R.D., M.P., A.T.V., L.M. performed animal experiments and analyzed data. E.C. contributed to the design and analyses of cell-based experiments and prepared the libraries for murine scRNAseq. F.D.Z, F.J., J.M. performed computational analyses on murine tissues. F.D.Z., F.J., J.M., D.N., and S.M. performed computational analyses on PSC patient tissues. T.F., S.Y., and T.H.K. provided liver

tissues of the Oslo cohort. M.H.'s laboratory performed IHC staining of mouse liver tissues. J.M.B., N.R., P.D., and C. S. provided important input into the MS. F.D.Z. and T.F.B. designed the figures and wrote the manuscript with edits from all the authors.

**Acknowledgements**

The authors acknowledge Marine Oudot, Sarah Durand, Cloé Gadenne, Nicolas Brignon, Romain Martin (all Inserm U1110, Strasbourg, France) and Danijela Heide (DKFZ Heidelberg, Germany) for excellent technical assistance, and Prof. A. Kramer (Universitätsspital Zürich) and Palak Trivedi (University of Birmingham) for helpful discussions. The authors acknowledge the Animal Experimentation Platform Infection and Cancer (ÆPIC) (University of Strasbourg, ITM Inserm UMR_S1110, Strasbourg, France) for the management of animal experiments.

**Data availability**

Transcriptomic data reported in this paper have been deposited at the GEO database with accession numbers GSE261990, GSE261991, and GSE261995.

**Financial support statement:**

The authors acknowledge the following financial support: European Research Council Grant ERC-AdG-2020 FIBCAN (T.F.B.); ARC Grant TheraHCC2.0 IHUARC, IHU201301187 (T.F.B.); French National Research Agency RHU DELIVER (ANR-21-RHUS-0001) and LABEX ANR-10-LABX-0028_HEPSYS (T.F.B.); the University of Strasbourg Foundation, the Alsace Cancer Foundation (T. F. B), the German Research Foundation (DFG) RO 5983/1-1 (N.R.). This work of the Interdisciplinary Thematic

Institute IMCBio, as part of the ITI 2021-2028 program of the University of Strasbourg, CNRS and Inserm, was further supported by IdEx Unistra (ANR-10-IDEX-0002), and by SFRI-STRAT'US project (ANR 20-SFRI-0012) and EUR IMCBio (ANR-17-EURE-0023) under the framework of the French Investments for the Future Program and the France 2030 program. JMB was funded by Spanish Carlos III Health Institute (ISCIII) [FIS PI18/01075, PI21/00922 and Miguel Servet Program CPII19/00008 to JMB) co-financed by the European Commission, and the European Union's Horizon 2020 Research and Innovation Program [ESCALON; grant number 825510]. ÆPIC was supported by University of Strasbourg IdEX 2024 "Dispositifs plateformes" (RDGGPJ2403M).

**Word count**: abstract: 273 (allowed 275), main text 5979 (allowed 6000, references, legends, included), number of references 32, number of figures 8 (allowed 8) + 12 Supplementary Figures.

**Impact and implications**

Primary sclerosing cholangitis (PSC) is a chronic fibrosing cholangiopathy with limited therapeutic options. Here, we identified the cell surface protein Claudin-1 as a mediator and therapeutic target for PSC. Claudin-1 expression in patients is associated with disease stage and outcome. A conditional liver epithelial-specific Claudin-1 knockout in mice resulted in reduced liver injury, fibrosis and cholestasis. Monoclonal antibodies targeting Claudin-1 inhibit fibrosis and cholestasis across state-of-the-art mouse models of PSC by inhibiting pro-inflammatory and fibrogenic signaling and the ductular reaction. The results of this preclinical study pave the way for the clinical development of Claudin-

1-specific antibodies for the treatment of PSC. It is therefore of impact for physicians, scientists and drug developers in the field of biliary disease.

## Abstract

**Background and aim:** Primary sclerosing cholangitis (PSC) is a cholangiopathy associated with high risk of development into end-stage liver disease and hepatobiliary cancer. The pathogenesis is poorly understood, and current clinical care offers limited therapeutic options, primarily relying on liver transplantation. Claudin-1 (CLDN1), a transmembrane protein highly expressed in liver epithelial cells, plays a crucial role in cell-cell communication and signaling. Here we aimed to investigate the functional role of CLDN1 as a mediator and therapeutic target for PSC using patient cohorts combined with murine and patient-derived intervention models. **Methods:** CLDN1 expression patterns and cell phenotypes were analyzed in liver tissues of five PSC patient cohorts using scRNAseq, spatial transcriptomics and multi-plex proteomics. Proof-of-concept studies using CLDN1-specific monoclonal antibodies (mAbs) and genetic loss-of-function were performed in state-of-the-art mouse models for PSC and cholangiopathies. Perturbation studies in human cell-based models were applied for mechanistic studies. **Results:** In liver tissues of patients with PSC, CLDN1 expression was highly up-regulated and associated with disease progression. Spatial transcriptomics and proteomics uncovered high expression of CLDN1 in diseased cholangiocytes and cholestatic periportal hepatocytes with concomitant upregulation of pro-inflammatory and profibrotic signaling pathways. Therapeutic administration of CLDN1-specific mAbs or genetic knock-out improved liver function in PSC mouse models by reducing hepatobiliary fibrosis and cholestasis. Mechanistic studies revealed that mAb treatment inhibited pro-inflammatory and pro-fibrotic signaling in cholangiocytes and hepatocytes perturbed in liver tissues of patients with PSC. **Conclusions:** Our results uncover a functional role of CLDN1 in the

pathogenesis of PSC and biliary fibrosis. Completed *in vivo* proof-of-concept studies combined with expression analyses in PSC patients pave the way for the clinical development of CLDN1-specific mAbs to treat PSC.

**Keywords:** antibody therapy**,** biliary fibrosis, cholangiopathies, signaling, proof-of-concept

## Introduction

Primary sclerosing cholangitis (PSC) is a progressive cholestatic liver disease of unknown origin. Genetic and autoimmune mechanisms have been suggested as predisposing factors, although the exact pathogenesis remains elusive.[1,2] The natural course of PSC leads to biliary fibrosis and strictures, resulting in chronic cholestasis and progressing to liver cirrhosis and failure. Liver cancer is a major complication of PSC at any stage. The risk of cholangiocellular carcinoma (CCA) is estimated at 20%.[3] Liver transplantation is the only therapeutic option available for patients with advanced disease, limited by recurrence in up to 25% of recipients.[3] Histological hallmarks of the disease are inflammation, fibrosis, cholestasis, and the ductular reaction, which is considered a mediator of disease progression.[4,5] While a large series of compounds have been investigated in clinical trials, none has shown to alter the natural progression of PSC.[1,6,7] The lack of approved disease-modifying drugs shows the high unmet clinical need for new therapeutic strategies.

CLDN1 is a transmembrane protein highly expressed in epithelial cells mediating cell-cell communication and signaling.[8] CLDN1 has been shown to play a functional role in the disease biology of inflammation, fibrosis and cancer.[8–11] In the liver, it is expressed in a junctional and nonjunctional (nj) form[9,10] exposed at the basolateral membrane of polarized hepatocytes, mediating liver fibrosis progressing to hepatocellular carcinoma (HCC).[8,9,12] We have previously developed monoclonal antibodies (mAbs) targeting a conformational epitope in the CLDN1 extracellular loop 1 comprising motif W(30)-GLW(51)-C(54)-C(64). The mAbs are highly specific for non-junctional CLDN1 without cross-reactivity to other Claudins.[13] In a metabolic dysfunction-associated steatohepatitis

(MASH)-driven HCC mouse model, mAb treatment inhibits liver fibrosis progressing to HCC with an excellent safety profile in non-human primates and healthy volunteers.[8,12,14] While patients with genetic CLDN1 mutations can present with sclerosing cholangitis,[15] the functional role of CLDN1 in PSC disease biology is unknown. Here, we investigated the functional role of CLDN1 as a mediator and therapeutic target in PSC.

## Materials and Methods

**Patient selection.** CLDN1 expression was investigated in five cohorts of patients with cholangiopathies. Liver transcriptomic datasets of patients with PSC and their respective controls were retrieved from ArrayExpress (EMBL-EBI), accession number E-GEOD-61260[16], and Gene Expression Omnibus (NIH), accession numbers GSE118373[4], GSE243981[17]. FFPE liver samples of patients with PSC were retrospectively obtained from the biobanks of the Norwegian PSC Research Center of Oslo, Norway (Table S1), the Department of Medicine and Surgery of the University of Milano-Bicocca, Italy (Table S2), and the University Hospital Leuven, Belgium (Table S3). Biopsies were assessed by an expert liver pathologist. The use of human samples was approved by the respective local ethical committees with informed patient consent.

**Computational analyses of patient samples.** Raw count matrices from microarray studies were pre-processed and normalized using the *oligo* package in R. scRNAseq PSC expression data[17] were analyzed using *Seurat*, *rstatix*, and *fgsea* packages in R. PSC spatial transcriptomics dataset[17] was analyzed using *Seurat* package in R. Detailed technical information is described in the supplementary material and methods.

**Immunohistochemistry, immunofluorescence, and multiple iterative labelling by antibody neodeposition (MILAN).** Detailed technical information is described in the supplementary material and methods.

**Antibodies**. Monoclonal anti-CLDN1 and IgG isotype control antibodies have been described.[8,18] Staining antibodies are described in Tables S5-S6.

**Animal experiments**. The bile duct ligation (BDL), DDC and Mdr2$^{-/-}$ mouse models,[19] expressing a human/mouse chimeric CLDN1 as a knock-in, were used to study the efficacy and safety of CLDN1 mAbs in vivo. Details are described in supplemental data.

**Bioinformatic and statistical analyses**. Bioinformatic procedures are described in supplementary data. Continuous data were compared using Student's t test when normally distributed (Shapiro-Wilk test) or non-parametric tests (Mann-Whitney U test and Kruskal-Wallis test) when non-normally distributed. Correlation was assessed by Spearman correlation test. Categorical data were analyzed using Fisher's Exact test. Outlier identification was carried out using the ROUT method (Q=1%). p-values<0.05 were considered statistically significant. Statistical analyses were performed using GraphPad Prism 9 and R.

## Results

**Claudin-1 expression is up-regulated in the liver of patients with PSC and correlates with disease progression.** To investigate the role of CLDN1 in clinical disease biology, CLDN1 expression was analyzed in PSC cohorts by immunohistochemistry (IHC) and quantitative proteomics at the single-cell level.

Furthermore, publicly available single cell[17], spatial[17], and bulk RNA transcriptomic[4,16] data sets of PSC patients were analyzed (Fig. 1-3).

*CLDN1* gene expression was markedly and significantly up-regulated in liver tissues of PSC patients, including the pro-fibrogenic ductular reaction (Fig. 1A). IHC staining of PSC samples from two well characterized cohorts (Milan, Oslo, Tables S1-2) revealed that CLDN1 protein up-regulation was robustly associated with disease progression (Fig. 1B, Tables S1-2), as shown by markedly increased CLDN1 expression with progressing liver fibrosis stage (Fig. 1B), independent of inflammatory bowel disease (IBD) co-morbidity (Fig.S1A). CLDN1 expression in patient liver tissues correlated with clinically validated prognostic scores including the Amsterdam-Oxford PSC score, the Mayo Risk Score for PSC, and the PREsTO score[20,21](Fig. 1C and S1B). CLDN1 expression also correlated with the magnitude of the ductular reaction (Fig. 1C), associated with poor prognosis in PSC.[5] Immunohistopathology analyses revealed that CLDN1 is robustly expressed in cholangiocytes lining damaged bile ducts as well as ductular reactive cells (Fig. 1D). Hepatocytes close to portal spaces showed elevated CLDN1 expression with a membranous pattern, likely in association with a cholestatic metaplastic phenotype (Fig. 1D). Multi-color fluorescent staining validated high CLDN1 protein expression in virtually all cytokeratin (CK) 19+ ductular cells in PSC liver tissues (Fig. 1E). Consistently, CLDN1 protein expression increased with disease progression from early to advanced fibrosis stages in non-cirrhotic PSC liver samples, along with ductular reactive cells and liver fibrotic content in immunohistochemistry analyses (Fig. 1F).

The marked upregulation of CLDN1 in PSC tissues, the expression of CLDN1 in PSC-driving cells, along with its association with disease progression suggest that CLDN1 plays a pathogenic role in PSC disease biology and is a therapeutic candidate target.

**Spatial transcriptomics and multi-plex proteomics in PSC patient liver tissues reveals co-localization of CLDN1 with known drivers of inflammation, fibrogenesis and stemness.** To investigate the biological role of CLDN1 in PSC progression, its expression in liver samples of PSC was investigated by single cell-resolved and spatial transcriptomics. At the single-cell level, the highest *CLDN1* expression levels were found in cells expressing markers of the biliary lineage, including cholangiocytes and biliary epithelial cells (Fig. 2A). An unbiased analysis of marker genes in CLDN1$^{High}$ cholangiocytes (Fig. 2B) revealed that top 4 differentially expressed genes included TNF-related weak inducer of apoptosis receptor (TWEAK receptor, *TNFRSF12A*), cytokeratin 7 (*KRT7)*, Chemokine (C-X-C motif) ligand 6 (*CXCL6*), and SRY-Box Transcription Factor 4 (*SOX4*) (Fig. 2B and Fig. S2A). Confirmatory studies at the protein level revealed that CLDN1+ CK19+ biliary epithelial cells were the major source of TNFα in PSC liver tissues (Fig. S2B). Gene set Enrichment Analysis (GSEA) of CLDN1$^{High}$ *vs* CLDN1$^{Low}$ differentially expressed genes revealed that high CLDN1 expression was associated with gene sets of bile duct proliferation, cholangitis, and senescence (Fig. 2C, left). Signaling pathways associated with CLDN1 expression included KRAS, NFκB, EMT, STAT3, and AKT (Fig. 2C, middle). Additionally, stemness-related gene sets were enriched in CLDN1$^{high}$ cholangiocytes (Fig. 2C, right). Analysis of a published spatial transcriptomics

dataset[17] revealed that *CLDN1* gene expression co-localized with the expression of known drivers of PSC, including *CDKN1A* (p21), NFκB effector *RELA* (p65), and *CXCL8* (IL-8), at the edges of PSC scar lesions (Fig. 2D). Interestingly, *CLDN1* expression correlated with the expression of pro-inflammatory and pro-fibrogenic genes, including *CXCL8* (Fig. 2E-F and Fig. S2C-D) and *CXCL6* and *MMP7* in transcriptomic regions neighboring high *CLDN1* expression (Fig. 2G and Fig. S2E). These findings suggest that high *CLDN1* expression is associated with expression of pro-inflammatory and pro-fibrogenic pathways.

To validate key findings of single cell gene expression at the protein level, 291'283 cells were phenotyped across samples of an independent cohort of PSC patients (Fig. 3A, Table S3) using multiplex spatial proteomic analysis based on Multiple Iterative Labeling by Antibody Neodeposition (MILAN).[22] Quantitative cytometry in PSC versus non-diseased tissues revealed a marked increase of CK19+CK7+ cholangiocytes including ductular reactive cells and CK18+CK7+CK19- intermediate epithelial cells such as dedifferentiating hepatocytes (Fig. 3B). A robust and significant increase of the total number of CLDN1+ cells in PSC compared to non-diseased liver tissues was observed (Fig. 3C), along with the increase of CLDN1 signal intensity per cell (Fig. 3D), validating the results obtained by immunohistochemistry (Fig. 1, 2) at single-cell resolution in an independent cohort. Protein expression analysis indicated co-localization of CLDN1 with mediators of biliary inflammation and fibrosis such as the pro-inflammatory cytokine TNFα, and immune and fibrosis modulator secreted phosphoprotein 1 (SPP1, osteopontin) in cholangiocytes and intermediate epithelial cells (Fig. 3E). CLDN1+TNFα+SPP1+ cells were observed surrounding to surround peri-biliary fibrotic

lesions (Fig. 3F-G, S3A-B), suggesting a potential role for CLDN1 in the biology of diseased cholangiocytes.

**Treatment with CLDN1-specific monoclonal antibodies improves liver function and survival by reducing fibrosis and cholestasis in state-of-the-art mouse models of PSC.** To study the functional role of CLDN1 in the disease biology of PSC and investigate the role of CLDN1 as a therapeutic target, proof-of-concept studies were performed in three complementary PSC animal models using highly specific CLDN1-specific antibodies.

Since the mAbs partially cross-react with mouse CLDN1,[8] we engineered a mouse model expressing a human/mouse (h/m) hybrid CLDN1 in all organs and cells where native CLDN1 is expressed. This was achieved by exchanging three amino acids in the mouse CLDN1 EL1-coding region using homologous recombination. The BDL model was applied first as it recapitulates cholestasis-driven fibrosis, as well as cholangiocyte reactivity and ductular reaction.[19,23] Forty 8-10 weeks-old male mice underwent surgical ligation of the common bile duct. Mice received 25 mg/kg CLDN1 mAb (n=20) or vehicle control (n=20) i.p. immediately after surgery and again on day 4 (Fig. 4A). Survival analysis of BDL mice showed that CLDN1 mAb treatment improved survival at day 7 (Fig. 4B). Liver function tests revealed an improvement of markers of liver injury, liver function, and cholestasis in CLDN1 mAb versus control-treated mice as shown by reduced levels of ALT, AST (Fig. 4C), total bilirubin and alkaline phosphatase (Fig. 4D). Bile acids remained unchanged (Fig. S4A). Furthermore, significantly increased levels of albumin (Fig. 4E) indicated liver function improvement. Automated analysis of the collagen proportionate area (CPA) (Fig. 4F-G, S4B) of Sirius Red-stained livers revealed a

significant reduction of liver fibrosis in CLDN1 mAb versus control-treated mice. Transcriptomic analyses revealed that CLDN1 mAb treatment modulated gene expression of fibrosis-related markers *Col1a1*, *Tgfb1, Acta2*, and *Timp1* in both RNAseq (Fig. 4H) and qPCR (Fig. S4C) analyses. Moreover, a robust reduction of the expression of markers of the ductular reaction including *Epcam*, *Krt19*, *Spp1* (Fig. 4I) and cytokeratin-7 (Fig. 4J) was observed. Additionally, CLDN1 mAb-treated mice exhibited reduced expression of pro-inflammatory cytokines (Fig. 4K).

Next, the DDC mouse model was applied, a chemical model for PSC recapitulating key features of sclerosing cholangitis and peribiliary fibrosis.[24] Forty 8-weeks-old male mice were fed with a 0.1% DDC-supplemented diet for four weeks. Following establishment of peri-biliary fibrosis in week 1,[24] mice were assigned 1:1 to receive weekly i.p. injections of 25 mg/kg CLDN1 mAb or vehicle control for three weeks (Fig. 5A). CLDN1 mAb treatment did not change survival (Fig. S5A) and decreased liver-to-body weight ratio (Fig. 5B). Analysis of liver function tests revealed significant decrease of plasma ALT (Fig. 5C), plasma bile acids (Fig. 5D) but not alkaline phosphatase (ALP)(Fig. S5B). Treatment with CLDN1 mAb resulted in a significant and robust reduction of liver fibrosis as shown by CPA analysis (Fig. 5E). CLDN1 treatment also resulted in inhibition of porto-portal bridging fibrosis – a key marker of disease progression in patients (Fig. 5F, S5C). The decreased expression of cytokeratin-19 (*Krt19*) and cytokeratin-7 indicated that CLDN1 mAb treatment reduced the ductular reaction (Fig. 5G). Analysis of differentially expressed genes by RNAseq and qPCR (Fig. S5D) revealed the downregulation of several pro-inflammatory mediators in CLDN1 mAb-treated mice (Fig. 5H and Fig. S5D). Confirming the histopathology findings, expression of genes involved

in fibrogenesis and extra-cellular matrix remodeling was significantly decreased, including fibulin 2 (*Fbln2*), integrin subunit beta 6 (*Itgb6*), matrix metallopeptidase 7 (*Mmp7*), matrix metallopeptidase 9 (*Mmp9*)(Fig. 5H), and transforming growth factor beta 2 (*Tgfb2*)(Fig. S5D).

Since CLDN1 has been shown to be up-regulated in the colon of patients with IBD,[25] the effect of CLDN1 mAb treatment on the colon was investigated. MAb treatment did not result in significant differences in colon length, colon weight, and intestinal permeability (Fig. S6A-E). Furthermore, no colon histopathological changes were observed, as previously shown for healthy mice across organs.[14] Treatment effects were similar in male and female mice (Fig. S6B and S7A-C), suggesting that there is likely no sex-dependency for CLDN1 mAb efficacy. A control group without diet served as a baseline to distinguish the specific effects of the diet from other variables (Fig. S7A-D). The effects of CLDN1 mAb were target-specific, since an isotype control did not show therapeutic effects (Fig. S7A-D). Moreover, CLDN1 mAb treatment did not modulate liver function tests in h/mCLDN1 KI mice under non-disease modeling conditions (Fig. S7D).

To further validate the functional role of CLDN1 in the pathogenesis of biliary fibrosis, the generation of an *Alb*.Cre/*Cldn1*$^{fl/fl}$ mouse model enabled investigation of biliary fibrosis development in mice with *Cldn1* conditional knock-out in liver epithelial cells. When challenged with 0.1% DDC feeding (Fig. 5I), *Alb*.Cre/*Cldn1*$^{fl/fl}$ robustly maintained the Cldn1 knock-out phenotype as shown by absence of CLDN1 expression in the liver (Fig. 5J), while exhibiting significantly less liver injury (Fig. 5K), less cholestasis (Fig. 5L), and less collagen deposition (Fig. 5M-N) compared to *Alb*.Cre controls.

The Mdr2$^{-/-}$ mouse model is a state-of-the-art model for PSC, as it recapitulates chronic disease progression modeling biliary fibrosis, cholestasis and hepatobiliary cancer, similar to the clinical course of PSC.[26] Mdr2$^{-/-}$ mice were treated in a therapeutic approach with CLDN1 mAb or control at the age of 6 weeks, when fibrosis and portal PSC–like lesions are already established.[26] After 12 weeks of treatment, mice were sacrificed, and plasma and livers harvested (Fig. 6A). While this model is characterized by low mortality, our data indicate that treatment with CLDN1 mAb improved survival compared to control animals (Fig. 6B). In a per-protocol analysis of relative weight change, CLDN1 mAb treatment significantly increased growth rate (Fig. 6C). CLDN1 mAb-treated Mdr2$^{-/-}$ mice exhibited a robust improvement of cholestasis as shown by reduced total bilirubin (Fig. 6D, S8A), plasma bile acids (Fig. 6D, S8B), and ALP (Fig. 6D). ALP levels, which are used as endpoints in clinical trials[1], were normalized in 73% of CLDN1 mAb-treated mice vs 28% of control-treated mice (Fig. 6D). The improvement of cholestasis was accompanied by reduced liver injury as shown by decreased AST and ALT levels (Fig. 6E). Importantly, CLDN1 mAb treatment resulted in reduced liver fibrosis including the inhibition of bridging fibrosis as shown by CPA analyses (Fig. 6F-G, S8C). The histopathological features of fibrosis reduction were accompanied by reduced gene expression of pro-inflammatory mediators (Fig. 6H). Analysis of cell fate marker expression revealed that CLDN1 mAb treatment downregulated biliary-fate marker SRY-Box Transcription Factor 9 (*Sox9*) while upregulating hepatic nuclear factor 4 alpha (*Hnf4a*) (Fig. 6I), while markers of the ductular reaction remained unchanged (Fig. S8D). The expression of extracellular matrix components collagen type IV alpha-1 chain

(*Col4a1*), collagen type V alpha-2 chain (*Col5a2*), and laminin subunit beta 1 (*Lamb1*) was significantly downregulated in CLDN1 mAb-treated mice (Fig. 6J, S8E).

Collectively, proof-of-concept studies in three state-of-the-art PSC mouse models showed improvement of CLDN1 mAb treatment on liver function, cholestasis, and fibrosis.

**CLDN1 mAb treatment inhibits pro-inflammatory and pro-fibrogenic signaling in PSC mouse and patient-derived models.** To investigate the mechanism of action of CLDN1 mAb treatment, liver gene expression from the three animal models was analyzed using RNAseq and compared with the perturbed liver transcriptome of PSC patients.[16] GSEA revealed that 1101 gene sets which were up-regulated in their expression in PSC patients were downregulated following CLDN1 mAb treatment across all mouse models (Fig. 7A). At the same time, 48 gene sets downregulated in PSC patients were restored in their expression across all mouse models (Fig. 7A). CLDN1 mAb treatment robustly suppressed the expression of PSC disease drivers and pathogenic signaling pathways (Fig. 7B). These included NFκB signaling, T cell receptor and macrophage signaling, TGFβ response, collagen formation as well as Notch and KRAS signaling and epithelial-to-mesenchymal transition (EMT). Of note, the suppression of bile acid metabolism in patients with PSC was also restored by CLDN1 mAb treatment. The perturbation of key pro-inflammatory and pro-fibrotic signaling pathways was validated in the BDL mouse model on the protein level using IHC and immunoblotting (Fig. 7C, S9A-B). CLDN1 mAb treatment significantly suppressed NFkB signaling as shown by decreased p65-positive area in reactive ductules in the BDL model in vivo (Fig. 7C), accompanied by marked reduction of nuclear p65 translocation (Fig. S9A). Moreover, CLDN1 treatment resulted

386 in inhibition of pro-fibrotic SRC, AKT and RAS signaling as shown by decreased
387 phosphorylation of SRC, AKT, and decreased RAS protein expression in immunoblot
388 analyses of mouse liver tissues treated with mAb (Fig. 7C, S9B). Since the majority of
389 these proteins have been shown to bind/interact with CLDN1 in the cell membrane[8,27] and
390 the CLDN1 antibody was not internalized following binding to the cholangiocyte cell
391 membrane (Fig. S10A-B), it is likely the mAb inhibits signaling by interfering with protein-
392 protein interactions at the cell membrane.

393 Liver scRNA-seq analysis of BDL mice informed of further mechanistic events
394 induced by antibody treatment at single-cell resolution (Fig. 8A). All the major liver cell
395 types were captured, hepatocytes, and macrophages being the most abundant cell types
396 (Fig. S9C). Given the CLDN1 expression profile in scRNA-seq and spatial transcriptomics
397 analyses in patients (Fig. 1, 2), we first focused on epithelial cell biology. CLDN1 mAb
398 treatment induced a significant downregulation of PSC-associated cholangiocyte and
399 hepatocyte marker genes (Fig. 8B). scGSVA analysis revealed that CLDN1 mAb
400 treatment reduced the expression of TNFα-NFκB, NOTCH1, AKT, and SRC signaling
401 pathways in both hepatocytes and cholangiocytes (Fig. 8C). The inhibition of
402 proinflammatory and pro-fibrogenic signaling was validated on the protein level where
403 CLDN1 mAb treatment modulated SRC, IKBα, and p65 phosphorylation (Fig. S11A-B) in
404 primary human cholangiocytes. The inhibition of epithelial cell signaling resulted in a
405 modulation of macrophage and myofibroblast functions, the effector cell types involved in
406 PSC and biliary fibrosis.[17,28] Single cell-resolved gene expression analysis of the pro-
407 fibrotic niche of the BDL mouse model revealed that CLDN1 mAb treatment suppressed
408 the expression of key pro-inflammatory and pro-fibrotic cytokines in nonparenchymal cells

(Fig. 8D) resulting in the suppression of the expression of major ECM components in fibroblasts, including *Col1a1* (Fig. 8D).

Collectively, these results unravel the targeted cell types and the mechanistic events, by which CLDN1 mAb treatment results in the improvement of cholestatic liver disease.

## Discussion

In this study, we identify CLDN1 as a previously undiscovered driver and therapeutic candidate target for PSC. This discovery is based on the following key findings: (1) CLDN1 is overexpressed in liver tissues of PSC patients and its level of expression correlates with disease progression (Fig. 1). (2) CLDN1 expression co-localizes with disease drivers and pathways in the diseased livers of PSC patients (Fig. 2-3). (3) A monoclonal antibody targeting exposed CLDN1 on cholangiocytes and hepatocytes reduces fibrosis, inflammation and cholestasis – hallmarks of PSC - in three state-of-the-art mouse models (Fig. 4-6). (4) A loss-of-function study using a liver-specific CLDN1 knock-out mouse model supports a functional role of CLDN1 in PSC disease biology (Fig. 5 I-N).

Mechanistically, our data are consistent with a model that CLDN1 overexpression in cholangiocytes and hepatocytes induces pro-inflammatory and pro-fibrogenic signaling (Fig. 7, 8E) resulting in the perturbation of epithelial cell fate and induction of the ductular reaction. Subsequent macrophage and fibroblast activation mediates inflammation, cholestasis and fibrosis (Fig. 7, 8F). Since the pathogenic role of the ductular reaction

and these signaling pathways have been well described in PSC disease biology,[5,8,29] it is likely that their inhibition mediates the effects of CLDN1 mAb treatment.

Our study has some limitations: first, we cannot exclude that other signaling pathways described for CLDN1 or additional mechanistic events are at play in mediating the effects of CLDN1 mAb. Second, although we used a large panel of complementary model systems for PSC disease biology, these model systems only partially recapitulate the complex pathogenesis of fibrosing cholangiopathies in patients (*e.g.* absence of IBD or intestinal biology). Third, analysis of fibrosis was limited to Sirius Red staining and collagen gene expression. Fourth, further studies will be needed to study whether CLDN1 mAb treatment will reduce the development of CCA in PSC-CCA models.

The overexpression of CLDN1 in PSC tissues across several patient cohorts combined with the robust effect of CLDN1 mAb treatment across three state-of-the-art in vivo models without detectable adverse events identify CLDN1 as previously undiscovered therapeutic target in PSC. The correlation of CLDN1 expression with disease biology (Fig. 1) identifies CLDN1 as a candidate biomarker for patient stratification. The modulation of secretory proteins TIMP1, metalloproteinases (Fig. 4 and 5) or CCL20, a cytokine associated with PSC[30] suppressed by antibody-treatment in all models (Fig. 4-6), provide opportunities for noninvasive target engagement markers in patients. Given the absence of approved therapeutic options and the limited success of compounds in clinical development, the treatment with CLDN1 mAb provides a new opportunity to improve the dismal prognosis of PSC patients.

Interestingly, we observed that the therapeutic effect of CLDN1 treatment on cholestasis, fibrosis and survival was most pronounced in the BDL model, suggesting that

454 BDL best models the pathways targeted by the antibody. Whether this finding eventually
455 translates to clinical treatment of patients e.g. large duct versus small duct disease or
456 major strictures remains to be determined.

457 A clinical challenge in PSC is the high risk of CCA and HCC and the lack of
458 effective surveillance. Since CLDN1 is overexpressed in CCA and HCC and CLDN1
459 mAbs have been shown to potently inhibit the development and growth of hepatobiliary
460 cancers in patient-derived tumor models,[8,12,31] it is likely that treatment with mAb will also
461 reduce the risk of CCA and HCC, key determinators for outcome and survival of PSC
462 patients. Furthermore, CLDN1 mAbs have been shown to be safe including non-human
463 primates[12] as well as healthy volunteers.[32] Collectively, the results of this study pave the
464 way for clinical development of CLDN1 mAbs as a first-in-class candidate treatment for
465 PSC.

466

467

## Figure Legends

**Fig. 1. CLDN1 is up-regulated in liver tissues from patients with PSC and correlates with disease progression**. (A) *CLDN1* gene expression in whole-liver tissues (Mann-Whitney, p=0.0175)(E-GEOD-61260)[16] and laser micro-dissected ductular reaction areas of patients with PSC (Mann-Whitney, p=0.0043)(GSE118373)[4]. (B) Quantification of CLDN1 expression in CLDN1-stained liver biopsies from two independent cohorts of patients with PSC, showing marked CLDN1 upregulation in patients, associated with fibrosis stage (Milan cohort: Mann-Whitney, p=0.009; Oslo cohort, continuous line indicates Kruskal-Wallis p=0.0036; dashed lines indicate pairwise Mann-Whitney: control vs Early-ALP$^{high}$ p=0.0286; control vs cirrhosis p=0.002; Early-ALP$^{low}$ vs cirrhosis p=0.008. (C) CLDN1 protein expression correlates with clinical prognostic scores, including the magnitude of the ductular reaction (Spearman's correlation, p=0.019, p=0.004, p=0.004, p=0.004, p=0.004, p=0.004, p=0.04, p=0.04 top to bottom). (D) Immunohistochemical staining on a PSC liver explant reveals strong CLDN1 expression in damaged bile ducts, ductular reaction, and cholestatic peri-portal hepatocytes. (E) Immunofluorescent staining showing robust CLDN1 expression in CK19-positive cells in PSC samples. Scale bars: 50 µm. (F) CLDN1 IHC staining of PSC samples at different stages, showing CLDN1 expression increasing along with disease stage, ductular reaction, and fibrotic content. * p<0.05; ** p<0.01; *** p<0.001; **** p<0.0001.

**Fig. 2. CLDN1 expression co-localizes with known PSC disease drivers in patients.** (A) In a published PSC scRNAseq atlas,[17] *CLDN1* is up-regulated in cholangiocytes of patients with PSC. (B) Differentially expressed genes (DEGs) analysis in PSC-derived

*CLDN1*$^{High}$ *vs CLDN1*$^{Low}$ biliary epithelial cells. Analysis of a spatial transcriptomic atlas of PSC.[17] (C) Pathway enrichment analyses revealed that *CLDN1*$^{High}$ biliary cells are characterized by distinct signaling, phenotype, and plasticity features compared to *CLDN1*$^{Low}$ counterparts. (D) Analysis of a spatial transcriptomic atlas of PSC[18]. *CLDN1* expression co-localizing with *CDKN1A*, *RELA*, and *CXCL8* at the interface of scar lesions. Insets show the interface region between a peri-biliary scar and surrounding non-fibrotic liver tissue. Dashed lines delineate a fibrotic scar. (E) Whole-PSC liver unbiased analysis of top 40 genes significantly correlating with *CLDN1* expression. (F) Top 20 genes significantly correlating with *CLDN1* expression in the 'Cholangiocyte' cluster. (G) Genes significantly correlating with *CLDN1* expression in a neighboring transcriptomic spot.

**Fig. 3. Spatial multiplex proteomics reveals an increase in CLDN1-expressing liver epithelial cells in PSC liver tissues at the single cell level.** (A) UMAP clustering of spatial proteomics-phenotyped liver tissue cells. (B) Quantitative cytometry shows increased numbers of cholangiocytes and intermediate epithelial cells in PSC compared to non-diseased livers (Mann-Whitney, $p<0.0001$). Expression of CK19+CK7+ was used to identify cholangiocytes including ductular reactive cells, staining of CK18+CK7+CK19- cells were used to identify intermediate epithelial cells such as dedifferentiating hepatocytes. (C) Quantitative cytometry shows increased numbers of CLDN1+ cells in PSC compared to non-diseased livers (Mann-Whitney, $p=0.0002$). (D) Quantitative cytometry showing increased CLDN1 staining intensity in CLDN1+ cells in PSC compared to non-diseased livers (Mann-Whitney, $p=0.0034$). (E) Protein expression of CLDN1, TNFα, and SPP1/Osteopontin in the cluster of cholangiocytes and intermediate epithelial

cells. (F) Digital reconstruction of representative TMA cores, phenotyped by spatial proteomics. (G) Individual panels showing representative TMA cores stained for CLDN1, CK19, SPP1, CLDN1+CK19+SPP1, and TNFα (upper to lower). *** p<0.001; **** p<0.0001.

**Fig 4. CLDN1 mAb treatment improves survival, liver function, cholestasis, and liver fibrosis in the bile duct ligation mouse model.** (A) Illustration of the experimental approach. (B) Survival analysis of bile-duct ligated mice revealed that CLDN1 mAb improved survival at 7 days (Log-rank test, p=0.08). (C-E) CLDN1 mAb treatment significantly ameliorated liver function tests, included ALT (Mann-Whitney, p=0.0163) and AST (Mann-Whitney, p=0.0185) (C), total bilirubin (Mann-Whitney, p=0.0118) and alkaline phosphatase (ALP, Mann-Whitney, p=0.0168) as markers of cholestasis (D), and albumin (Mann-Whitney, p=0.0006) as marker of liver biosynthetic function (E). (F) CLDN1 mAb treatment reduced fibrosis levels as measured by Sirius Red Collagen Proportionate Area (Mann-Whitney, p<0.0001). (G) Representative images of Sirius Red-stained livers of control and CLDN1 mAb-treated mice. Scale bars: 500 µM. (H-K) Expression of fibrosis (H), cell-fate and ductular reaction (I-J) and inflammation (K) markers in the livers of control and CLDN1 mAb-treated mice (*Col1a1*: p=0.0079; *Tgfb1*: p=0.0079; *Acta2*: p=0.0317; *Timp1*: p=0.0079, *Krt19*: p=0.0056; *Spp1*: p=0.0011; Ck7: p=0.0357; *Ccl24*: p=0.0079; *Tnf*: p=0.0079; *Il1b*: p=0.0079; Mann-Whitney). Scale bars: 250 µM. * p<0.05; ** p<0.01; *** p<0.001; **** p<0.0001. AST (C, right) and bilirubin (D, left) panels show n=7 control and n=10 CLDN1 mAb-treated mice. The plasma of 8 control and 5 treated mice could not be analyzed due to hemolysis interfering with analyte

measurements. Data in (H) and (K) were obtained from RNAseq analyses of a subset of 5 representative liver tissues (n=5 vs n=5).

**Fig. 5. CLDN1 mAb treatment ameliorates liver injury and fibrosis in the DDC mouse model.** (A) Illustration of the experimental approach. (B) Analysis of the liver index (liver-to-body weight ratio) suggesting reduced cell proliferation in treated mice (Mann-Whitney, p=0.0055). (C) CLDN1 mAb treatment ameliorated liver injury as shown by decreased levels of alanine aminotransferase (ALT)(Mann-Whitney, p=0.0009). (D) CLDN1 mAb treatment reduced cholestasis as measured by plasma concentrations of bile acids (Mann-Whitney, p=0.0559). (E) CLDN1 mAb treatment reduced fibrosis levels as measured by Sirius Red Collagen Proportionate Area (Mann-Whitney, p<0.0001). (F) Representative images of Sirius Red-stained livers of control and CLDN1 mAb-treated mice. Scale bars: 500 µM. (G) CLDN1 mAb treatment reduced the magnitude of ductular reaction, as measured by *Krt19* gene expression (Mann-Whitney, p=0.0777) and cytokeratin-7 immunostaining (Mann-Whitney, p=0.0159). Scale bars: 250 µM. (H) Liver expression (RNAseq analyses of 5 liver tissues of each group, n=5 vs n=5) of genes encoding for inflammation and fibrosis markers (*Ccl20*: p=0.0079; *Ccl17* p=0.0079; *Cxcl5*: p=0.0079; *Fbln2*: p=0.0079, *Itgb6*: p=0.0159; *Mmp7*: p=0.0317; *Mmp9*: p=0.0079; Mann-Whitney). (I) Experimental approach of *Alb*.Cre/*Cldn1*$^{fl/fl}$ mice with conditional *Cldn1* knock-out in liver epithelial cells and subjected to DDC diet. (J) Liver Cldn1 expression in *Alb*.Cre and *Alb*.Cre/*Cldn1*$^{fl/fl}$ mice, validating the loss of CLDN1 expression in DDC feed KO mice. (K) Plasma ALT (Mann-Whitney, p=0.0039) and (L) ALP (Mann-Whitney, p=0.2799) levels were decreased in *Alb*.Cre/*Cldn1*$^{fl/fl}$ mice. (M) Cldn1 knock-out in liver

epithelial cells significantly reduced fibrosis development in the DDC mouse model (Mann-Whitney, p=0.0011). (N) Representative images of Sirius Red-stained liver of *Alb*.Cre and *Alb*.Cre/Cldn1$^{fl/fl}$ mice. Scale bars: 500 µM. * p<0.05; ** p<0.01; *** p<0.001; **** p<0.0001.

**Fig. 6. CLDN1 mAb treatment improves survival, liver function, and liver fibrosis in the Mdr2$^{-/-}$ mouse model.** (A) Illustration of the experimental approach. (B) Survival analysis of Mdr2$^{-/-}$ mice revealing improved survival in CLDN1 mAb-treated group (log-rank test, p=0.0887). (C) Increased growth rate in CLDN1 mAb-treated Mdr2$^{-/-}$ mice (extra sum-of-squares F-test, p<0.0001). Error bars: mean ± SEM. (D) CLDN1 mAb treatment significantly decreased markers of cholestasis (Bilirubin: p=0.0023; Bile acids: p=0.0519, Mann-Whitney, and ALP: p=0.077, t-test), resulting in the normalization of plasma ALP levels in 73% of mice (Fisher's exact test, p=0.01). (E) Plasma levels of AST (Mann-Whitney, p=0.0242) and ALT (Mann-Whitney, p=0.0936) as markers of liver injury were reduced in CLDN1 mAb-treated group. (F) CLDN1 mAb treatment reduced fibrosis levels as measured by Sirius Red Collagen Proportionate Area (Mann-Whitney, p<0.0001). (G) Representative images of Sirius Red-stained livers of control and CLDN1 mAb-treated mice. Scale bars: 500 µm. (H-J) Liver gene expression (RNAseq, n=5 vs n=5) of key inflammation (H), cell fate (I), and fibrosis markers (J). (*Ccl20*: p=0.0317; *Ccl12* p=0.0317; *Tlr4*: p=0.0159; *Sox9*: p=0.0159, *Hnf4a*: p=0.0079; *Col4a1*: p=0.0317; *Col5a2*: p=0.0317; *Lamb1*: p=0.0317, Mann-Whitney). * p<0.05; ** p<0.01; **** p<0.0001. Bilirubin (D, left) and AST (E, left) panels show n=14 control and n=21 CLDN1 mAb-treated mice. The

plasma of 4 control and 1 treated mice could not be analyzed due to hemolysis interfering with analyte measurements.

**Fig. 7. CLDN1 mAb treatment suppresses pro-inflammatory, pro-fibrotic and pro-carcinogenic signaling pathways *in vivo*.** (A) Venn diagrams of pathways differentially enriched in the livers of patients with PSC and in the liver of mouse models. (B) Comparison of PSC liver transcriptome with transcriptomic changes induced by CLDN1 mAb treatment in mouse models. Heatmaps illustrate NES of representative altered gene sets, each condition versus their respective control. (C) Quantification of IHC and immunoblot signals validating transcriptomic findings on the protein level in the BDL mouse model (NFκB-p65: p=0.0004; AKT: p<0.0001; SRC: p=0.0475; RAS: p=0.0226, Mann-Whitney). * p<0.05; ** p<0.01; *** p<0.001; **** p<0.0001.

**Fig. 8. CLDN1 mAb treatment suppresses pro-inflammatory and pro-fibrotic signaling in liver epithelial cells with inhibition of macrophage and fibroblast activation.** (A) scRNA-Seq clustering of livers from the BDL mouse model. (B) scGSVA enrichment analysis of gene signatures of PSC cholangiocytes and PSC hepatocytes (Mann-Whitney, both p<0.0001). (C) scGSVA enrichment analysis of TNF-NFkB, SRC, NOTCH1, and AKT signaling pathways (Mann-Whitney, all p<0.0001). (D) Cell type-specific gene expression of key mediators of the pro-fibrotic niche in biliary fibrosis, showing CLDN1 mAb ultimate effect on collagen production by myofibroblasts (Mann-Whitney, all p<0.0001). (E) Mechanistic model of CLDN1 mAb-mediated inhibition of liver

604 and biliary signaling based on transcriptomic and proteomic analyses. (F) Mechanistic
605 model of CLDN1 mAb-mediated anti-fibrotic and anti-inflammatory efficacy in preclinical
606 models for PSC based on scRNA-Seq analyses. * $p<0.05$; ** $p<0.01$; *** $p<0.001$; ****
607 $p<0.0001$.

608

## References

[1] Vesterhus M, Karlsen TH. Emerging therapies in primary sclerosing cholangitis: pathophysiological basis and clinical opportunities. J Gastroenterol 2020;55:588–614.

[2] Karlsen TH, Folseraas T, Thorburn D, et al. Primary sclerosing cholangitis - a comprehensive review. J Hepatol 2017;67:1298–1323.

[3] Dyson JK, Beuers U, Jones DEJ, et al. Primary sclerosing cholangitis. Lancet 2018;391:2547–2559.

[4] Govaere O, Cockell S, Van Haele M, et al. High-throughput sequencing identifies aetiology-dependent differences in ductular reaction in human chronic liver disease. J Pathol 2019;248:66–76.

[5] Carpino G, Cardinale V, Folseraas T, et al. Hepatic Stem/Progenitor Cell Activation Differs between Primary Sclerosing and Primary Biliary Cholangitis. Am J Pathol 2018;188:627–639.

[6] Bowlus CL, Arrivé L, Bergquist A, et al. AASLD practice guidance on primary sclerosing cholangitis and cholangiocarcinoma. Hepatology 2023;77:659–702.

[7] European Association for the Study of the Liver. Electronic address: easloffice@easloffice.eu, European Association for the Study of the Liver. EASL Clinical Practice Guidelines on sclerosing cholangitis. J Hepatol 2022;77:761–806.

628 [8] Roehlen N, Saviano A, El Saghire H, et al. A monoclonal antibody targeting
629 nonjunctional claudin-1 inhibits fibrosis in patient-derived models by modulating cell
630 plasticity. Sci Transl Med 2022;14:eabj4221.

631 [9] Zeisel MB, Dhawan P, Baumert TF. Tight junction proteins in gastrointestinal and
632 liver disease. Gut 2019;68:547–561.

633 [10] Nehme Z, Roehlen N, Dhawan P, et al. Tight Junction Protein Signaling and Cancer
634 Biology. Cells 2023;12:243.

635 [11] Hasegawa K, Wakino S, Simic P, et al. Renal tubular Sirt1 attenuates diabetic
636 albuminuria by epigenetically suppressing Claudin-1 overexpression in podocytes.
637 Nat Med 2013;19:1496–1504.

638 [12] Roehlen N, Muller M, Nehme Z, et al. Treatment of HCC with claudin-1-specific
639 antibodies suppresses carcinogenic signaling and reprograms the tumor
640 microenvironment. J Hepatol 2022:S0168-8278(22)03147–6.

641 [13] Fofana I, Krieger SE, Grunert F, et al. Monoclonal anti-claudin 1 antibodies prevent
642 hepatitis C virus infection of primary human hepatocytes. Gastroenterology
643 2010;139:953–964, 964.e1–4.

644 [14] Mailly L, Xiao F, Lupberger J, et al. Clearance of persistent hepatitis C virus infection
645 in humanized mice using a claudin-1-targeting monoclonal antibody. Nat Biotechnol
646 2015;33:549–554.

[15] Hadj-Rabia S, Baala L, Vabres P, et al. Claudin-1 gene mutations in neonatal sclerosing cholangitis associated with ichthyosis: a tight junction disease. Gastroenterology 2004;127:1386–1390.

[16] Horvath S, Erhart W, Brosch M, et al. Obesity accelerates epigenetic aging of human liver. Proc Natl Acad Sci U S A 2014;111:15538–15543.

[17] Andrews TS, Nakib D, Perciani CT, et al. Single-cell and spatial transcriptomics characterisation of the immunological landscape in the healthy and PSC human liver. J Hepatol 2024:S0168-8278(24)00003–5.

[18] Colpitts CC, Tawar RG, Mailly L, et al. Humanisation of a claudin-1-specific monoclonal antibody for clinical prevention and cure of HCV infection without escape. Gut 2018;67:736–745.

[19] Mariotti V, Strazzabosco M, Fabris L, et al. Animal models of biliary injury and altered bile acid metabolism. Biochim Biophys Acta Mol Basis Dis 2018;1864:1254–1261.

[20] Mazhar A, Russo MW. Systematic review: non-invasive prognostic tests for primary sclerosing cholangitis. Aliment Pharmacol Ther 2021;53:774–783.

[21] Goet JC, Floreani A, Verhelst X, et al. Validation, clinical utility and limitations of the Amsterdam-Oxford model for primary sclerosing cholangitis. J Hepatol 2019;71:992–999.

[22] Antoranz A, Van Herck Y, Bolognesi MM, et al. Mapping the Immune Landscape in Metastatic Melanoma Reveals Localized Cell-Cell Interactions That Predict Immunotherapy Response. Cancer Res 2022;82:3275–3290.

[23] Georgiev P, Jochum W, Heinrich S, et al. Characterization of time-related changes after experimental bile duct ligation. Br J Surg 2008;95:646–656.

[24] Fickert P, Stöger U, Fuchsbichler A, et al. A new xenobiotic-induced mouse model of sclerosing cholangitis and biliary fibrosis. Am J Pathol 2007;171:525–536.

[25] Pope JL, Bhat AA, Sharma A, et al. Claudin-1 regulates intestinal epithelial homeostasis through the modulation of Notch-signalling. Gut 2014;63:622–634.

[26] Popov Y, Patsenker E, Fickert P, et al. Mdr2 (Abcb4)-/- mice spontaneously develop severe biliary fibrosis via massive dysregulation of pro- and antifibrogenic genes. J Hepatol 2005;43:1045–1054.

[27] Kovalski JR, Bhaduri A, Zehnder AM, et al. The Functional Proximal Proteome of Oncogenic Ras Includes mTORC2. Mol Cell 2019;73:830-844.e12.

[28] Lei L, Bruneau A, El Mourabit H, et al. Portal fibroblasts with mesenchymal stem cell features form a reservoir of proliferative myofibroblasts in liver fibrosis. Hepatology 2022;76:1360–1375.

[29] Fiorotto R, Villani A, Kourtidis A, et al. The cystic fibrosis transmembrane conductance regulator controls biliary epithelial inflammation and permeability by regulating Src tyrosine kinase activity. Hepatology 2016;64:2118–2134.

[30] Ellinghaus D, Jostins L, Spain SL, et al. Analysis of five chronic inflammatory diseases identifies 27 new associations and highlights disease-specific patterns at shared loci. Nat Genet 2016;48:510–518.

[31] Muller M, Nehme Z, Roehlen N, et al. Abstract #202 - Treatment of cholangiocarcinoma with a humanized anti-Claudin-1 monoclonal antibody. Hepatology 2022;76:S1–S1564.

[32] Alentis Therapeutics. Alentis Therapeutics reports positive topline results from pahese 1 multiple ascending dose cohort study. Press release Alentis Therapeutics 2023. Available at: https://alentis.ch/alentis-therapeutics-reports-positive-topline-results-from-phase-1-multiple-ascending-dose-cohorts-study/ [Accessed September 27, 2023].

# Fig. 1



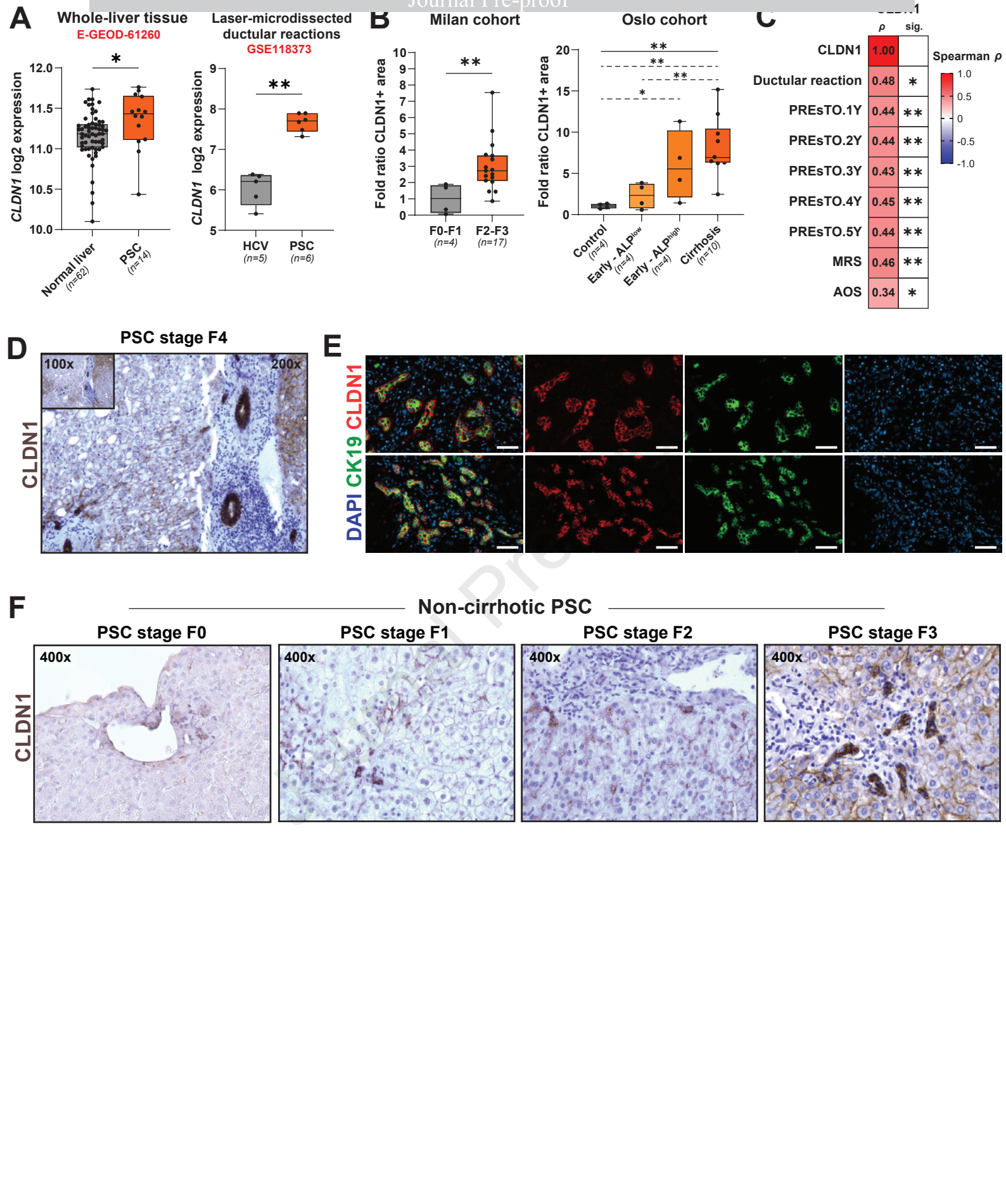

# Fig. 2



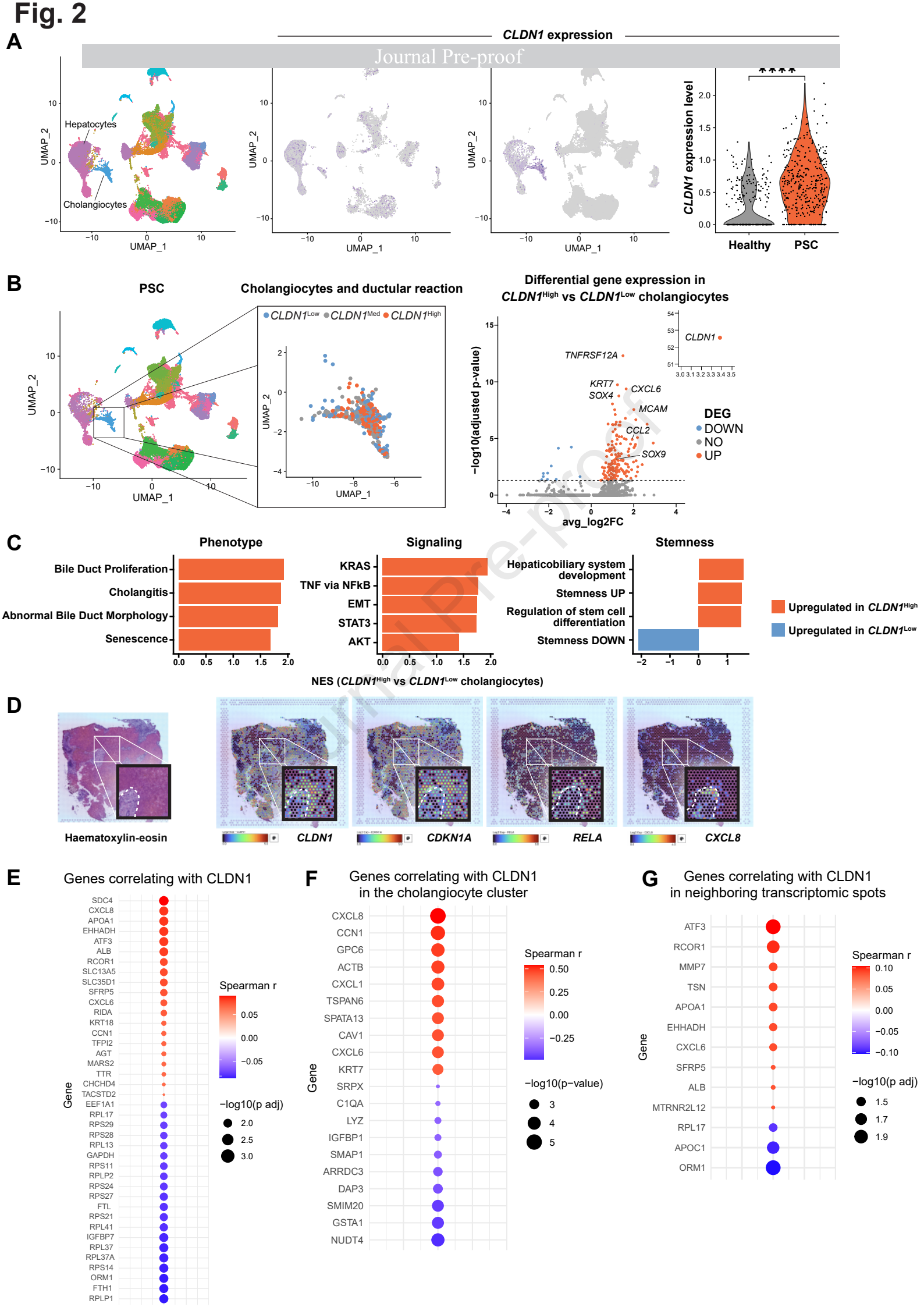

# Fig. 3



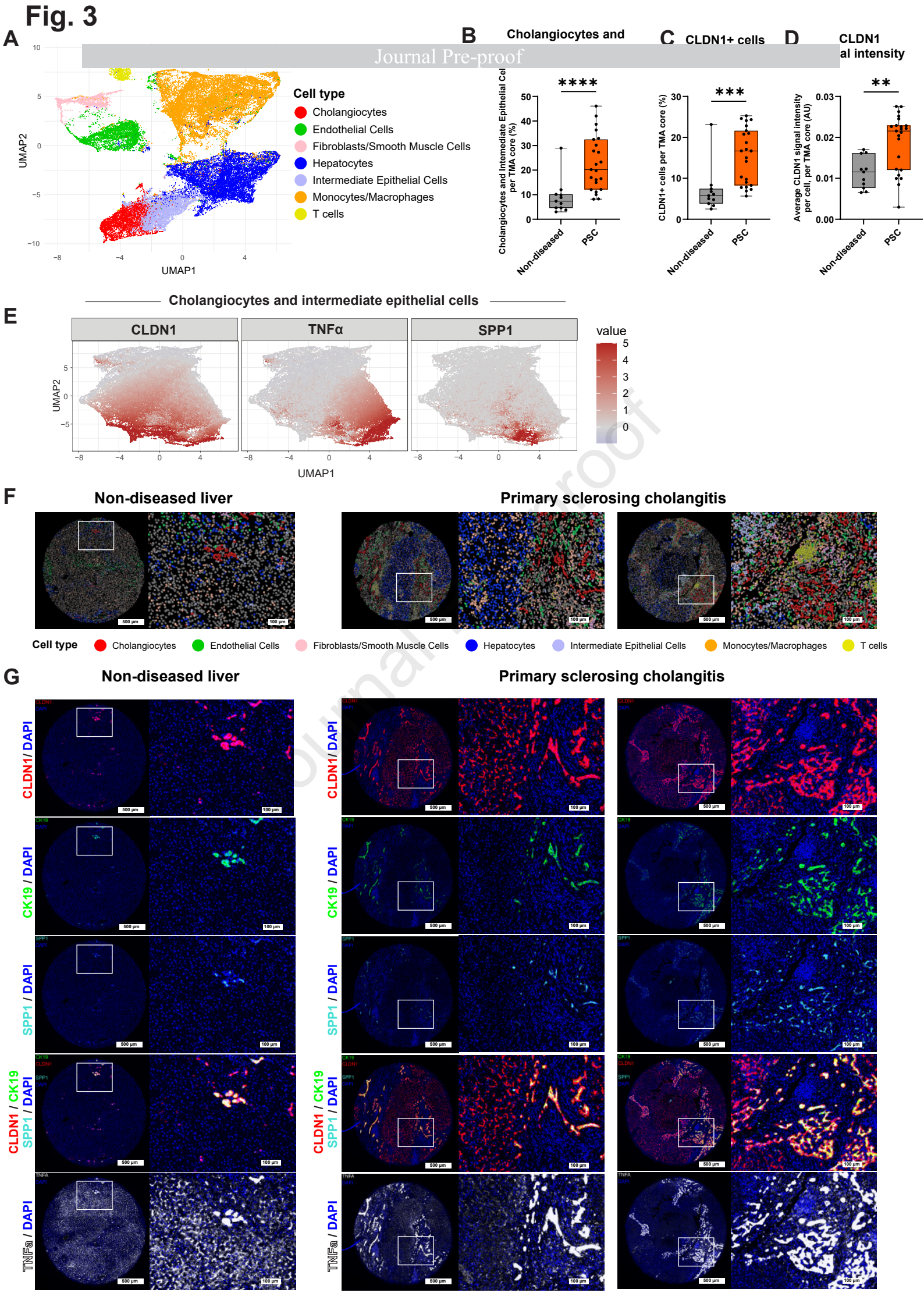

# Fig. 4



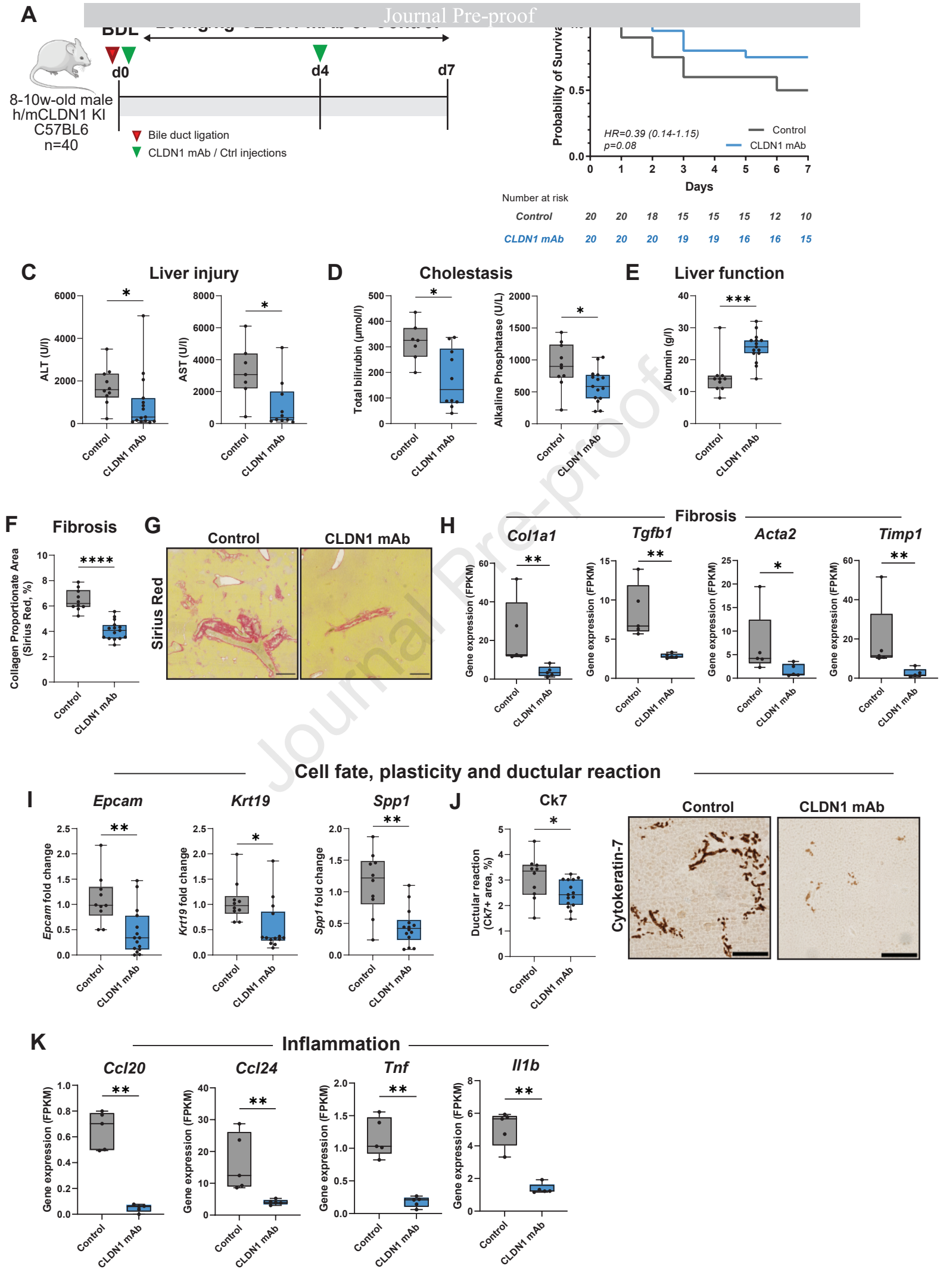

# Fig. 5



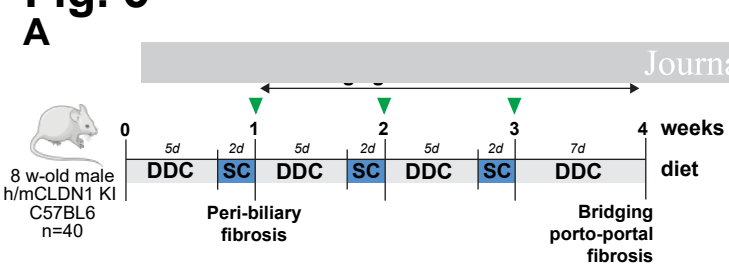


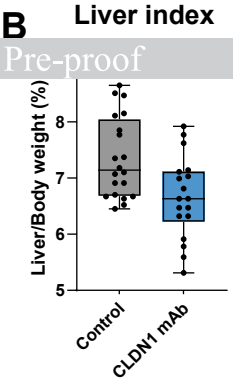


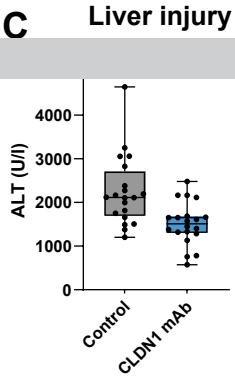


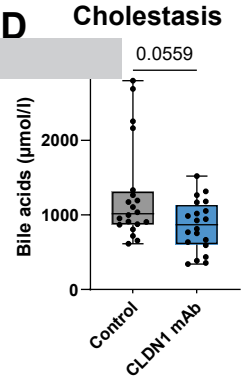


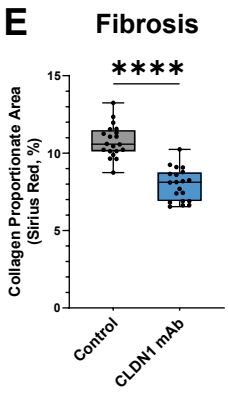


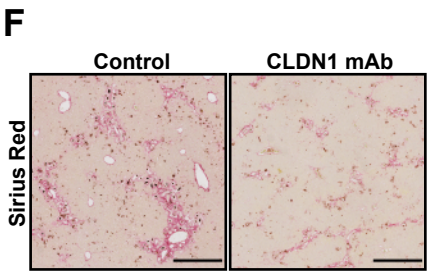


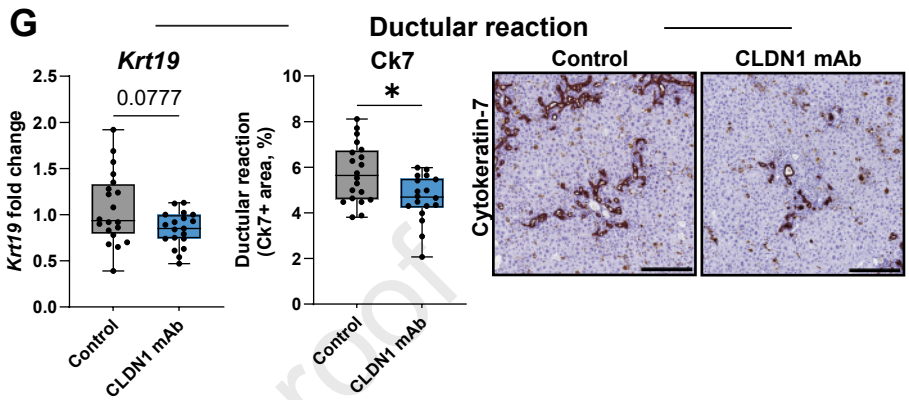


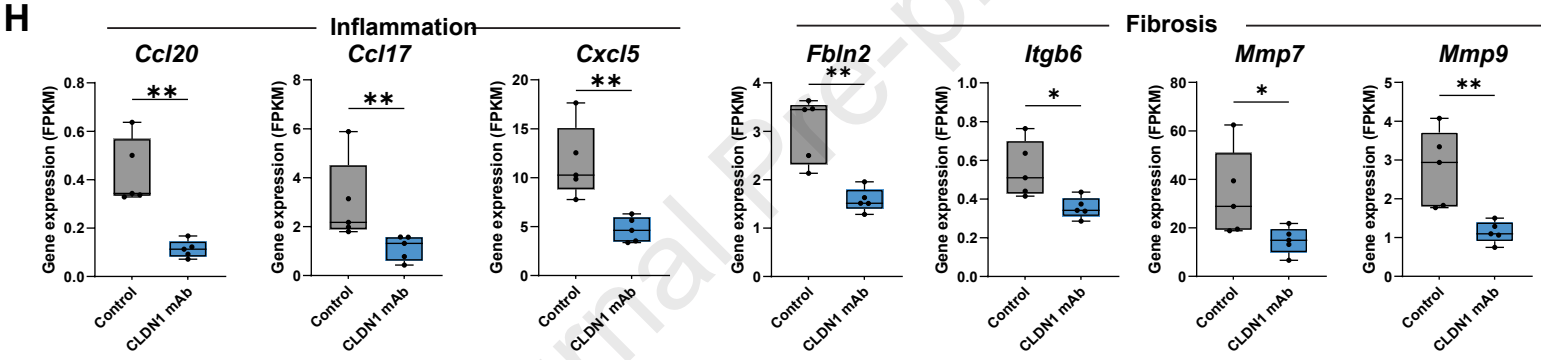


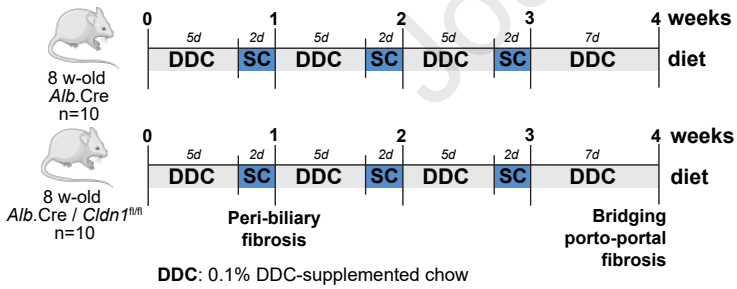


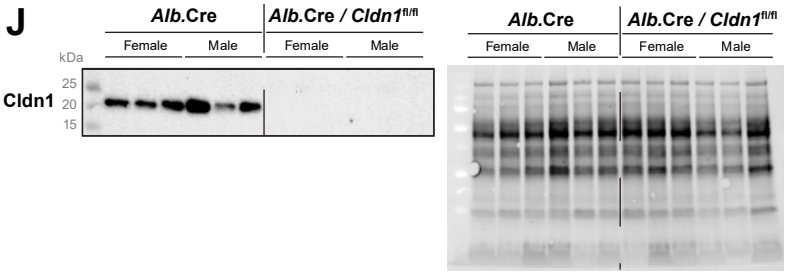


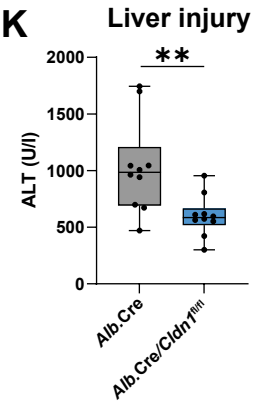


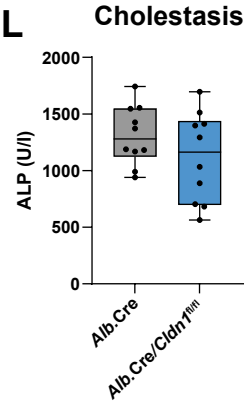


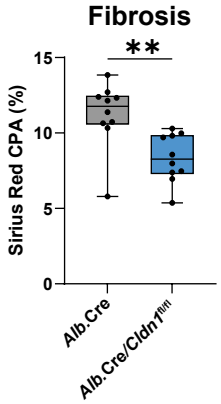


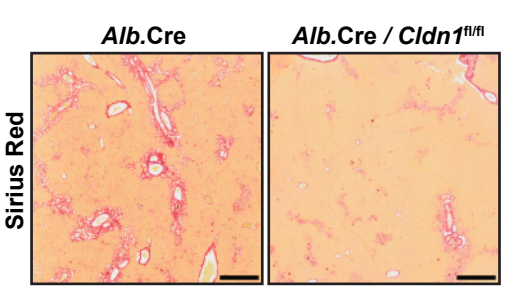

# Fig. 6



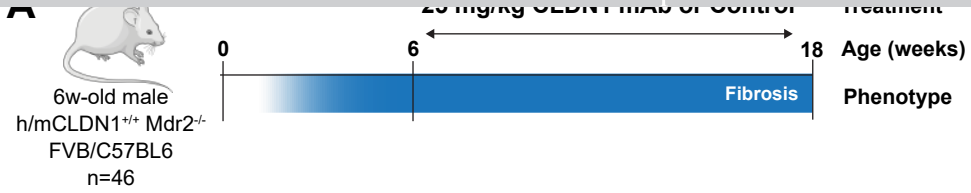


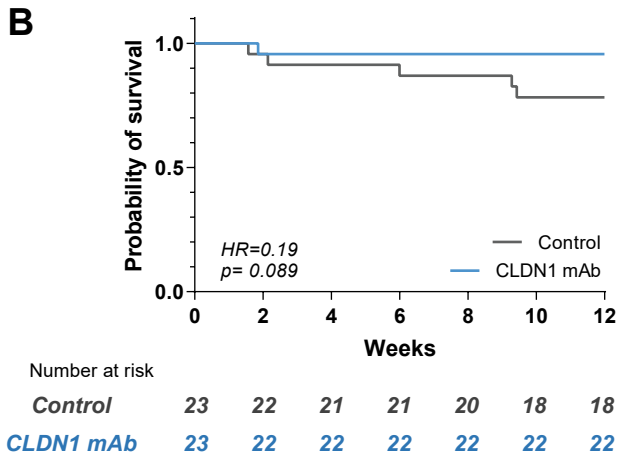


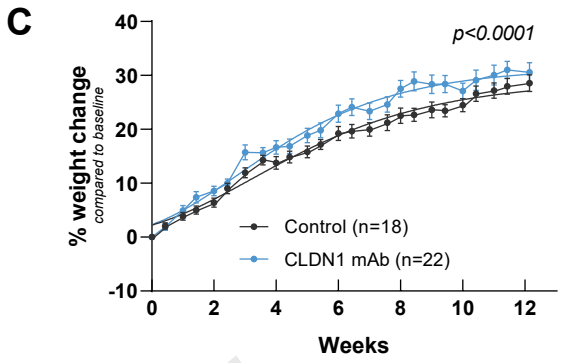


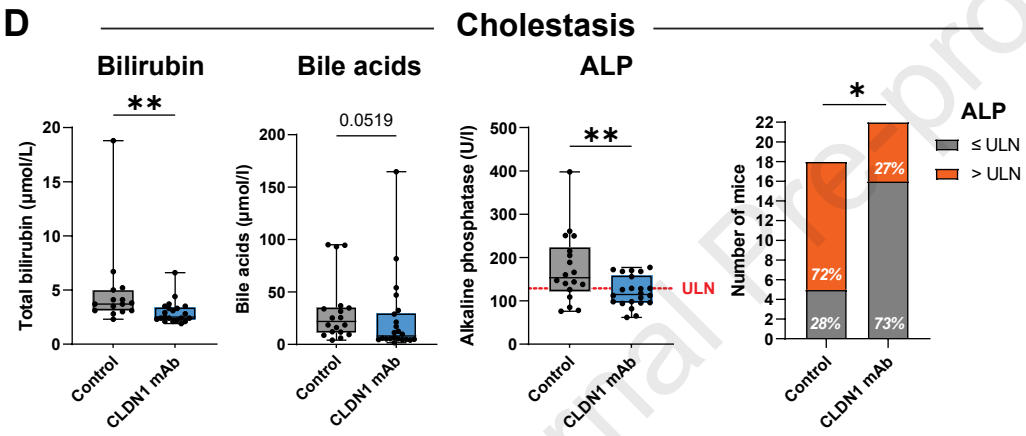


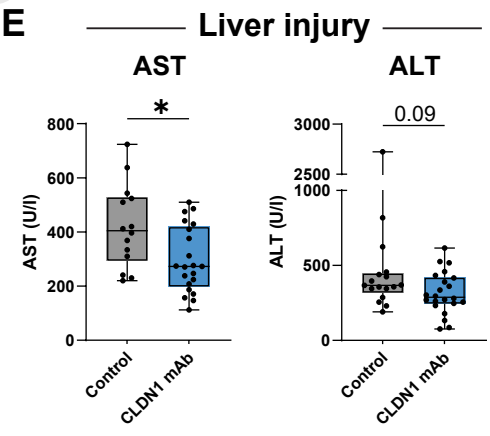


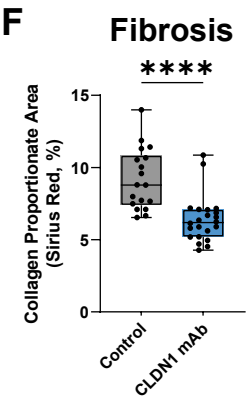


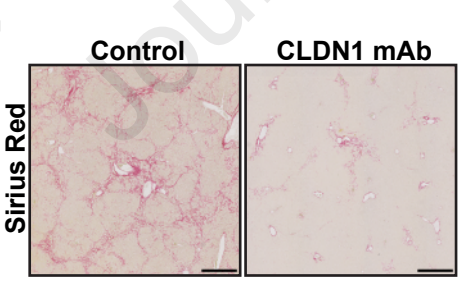


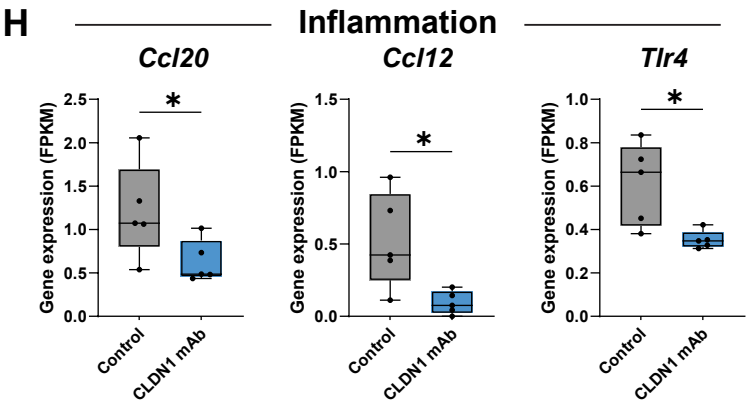


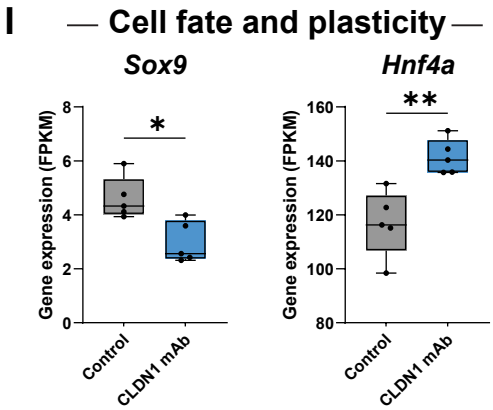


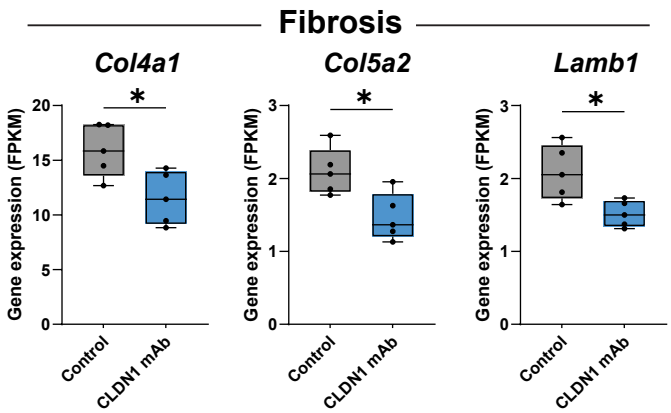

# Fig. 7



**A**

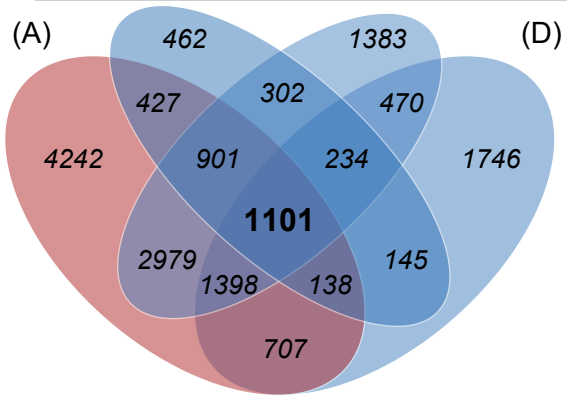


(A): upregulated in PSC vs healthy liver
(B): downregulated by CLDN1 mAb in DDC mice
(C): downregulated by CLDN1 mAb in BDL mice
(D): downregulated by CLDN1 mAb in Mdr2$^{-/-}$ mice

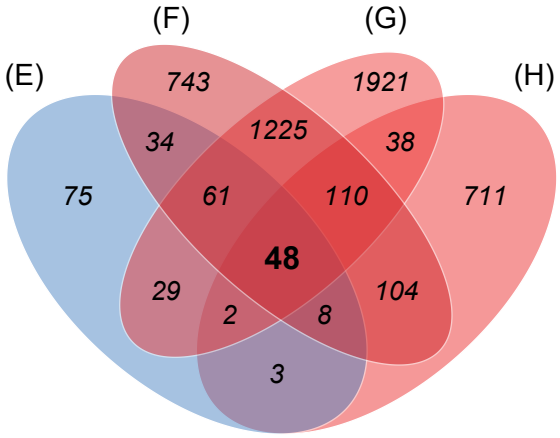


(E): downregulated in PSC vs healthy liver
(F): upregulated by CLDN1 mAb in DDC mice
(G): upregulated by CLDN1 mAb in BDL mice
(H): upregulated by CLDN1 mAb in Mdr2$^{-/-}$ mice

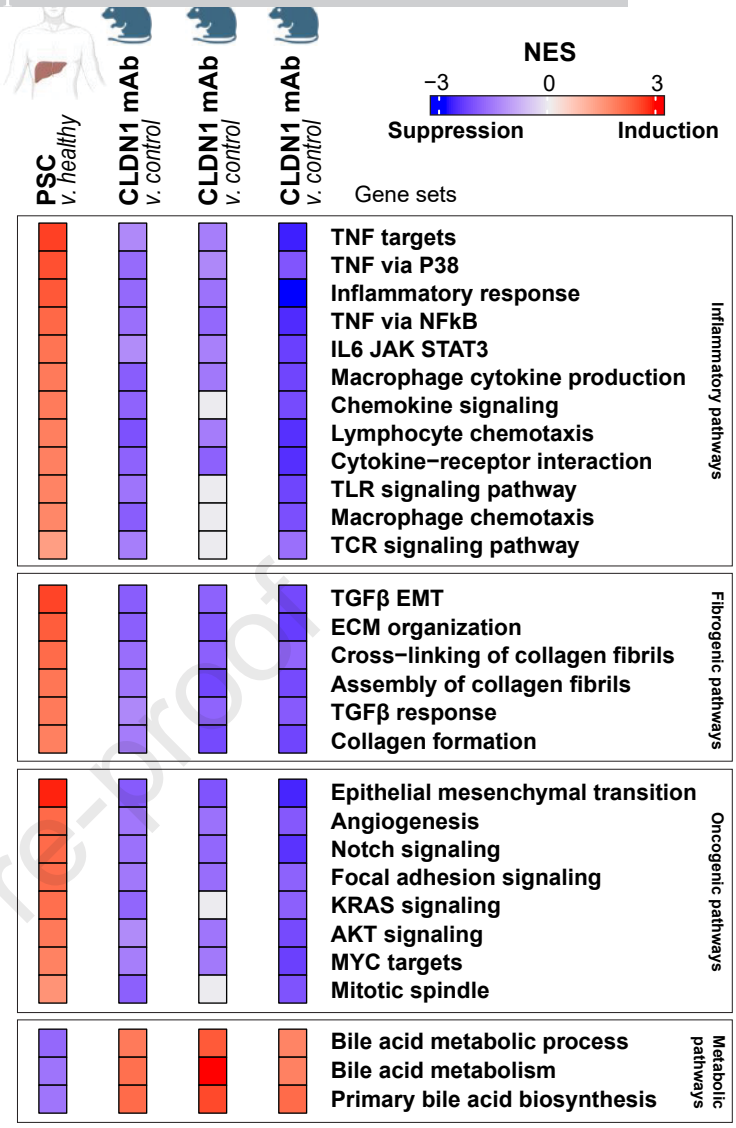


**C**

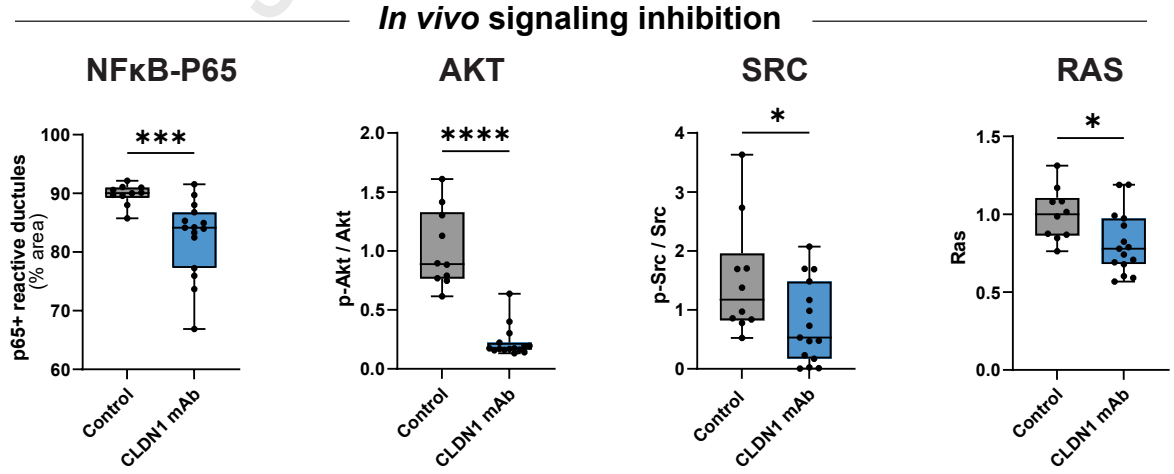

# Fig. 8



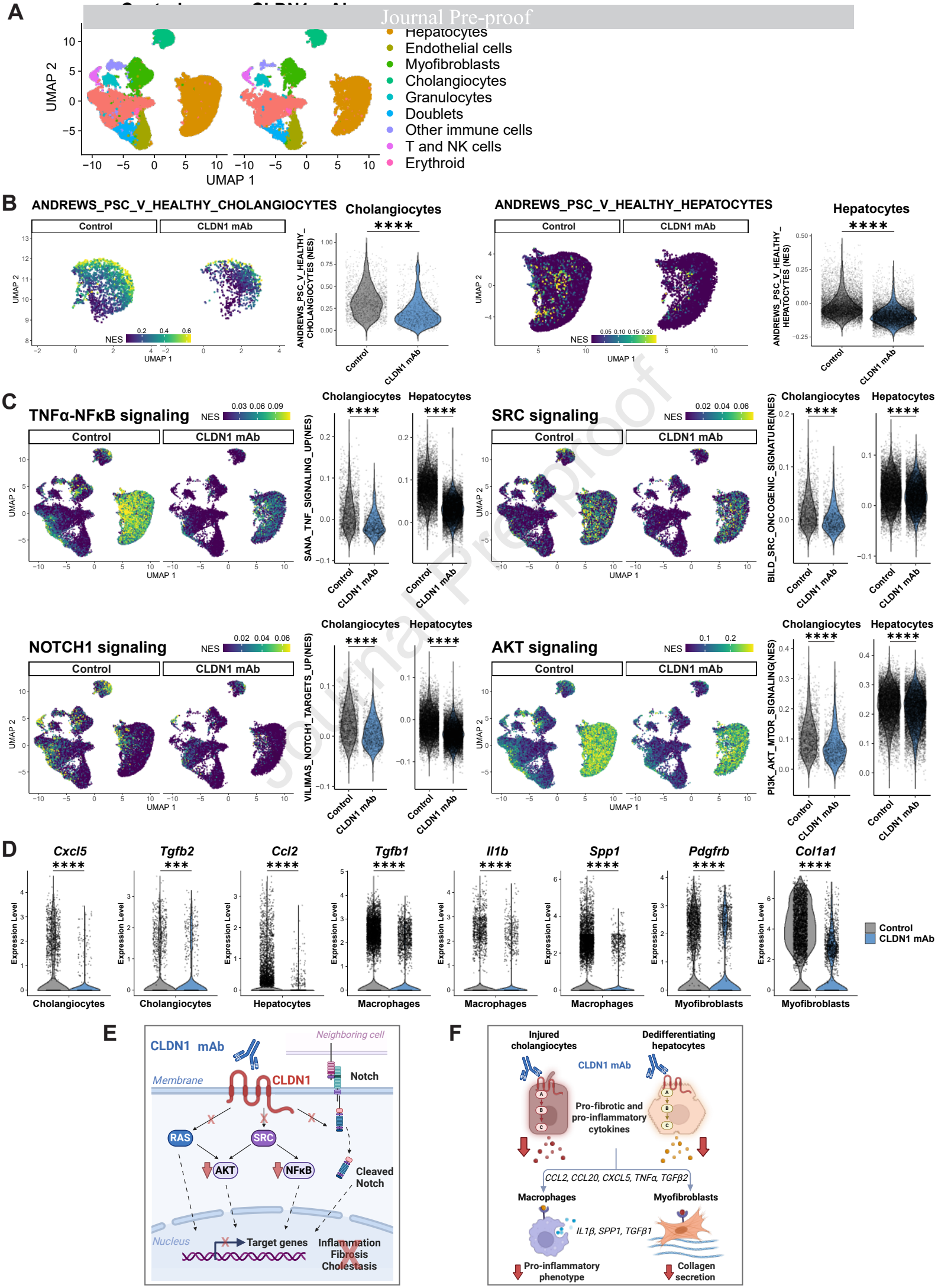

## Highlights

- Claudin-1 is overexpressed in PSC cholangiocytes and its expression correlates with PSC prognosis in patients
- Spatial transcriptomics, proteomics, and loss-of-function studies unravel Claudin-1 as disease driver
- Treatment with a Claudin-1-specific monoclonal antibody improves survival, fibrosis, inflammation and cholestasis in PSC mouse models
- Claudin-1 antibodies inhibit profibrotic and proinflammatory signaling in cholangiocytes
- Completed preclinical proof-of-concept offers the perspective for an effective and safe first-in-class treatment in patients.